SAND2016-9949C

Novel Particle Release Patterns for Increased Receiver Thermal Efficiency

Brantley Mills, Clifford K. Ho,[a)] Joshua M. Christian, and Gregory Peacock

Sandia National Laboratories, P.O. Box 5800, MS-1127, Albuquerque, NM 87185-1127, USA

[a)]*Corresponding author: ckho@sandia.gov*

Abstract. Novel particle release patterns have been investigated for falling particle receivers. Zig-zag, wave-like, and multiple parallel particle curtains have been simulated and compared to a conventional planar particle curtain. Simulations show that particle release patterns that promote light-trapping through non-planar features and volumetric heating can increase the thermal efficiency of particle receivers by nearly 10%, despite an increase in convective heat loss. Multiple parallel curtains yielded the highest efficiencies overall, while larger amplitudes and high frequencies in the wave-like patterns yielded high efficiencies relative to the baseline planar case. Thermal efficiency increased with increasing mass flow rate for all cases (up to 12.5 kg/s-m), while the relative improvement of the alternative release patterns decreased relative to the baseline. Testing has demonstrated the ability to implement these alternative release patterns using discharge plates that have machined slots of the desired pattern.

INTRODUCTION

Falling particle receivers are being studied to achieve higher temperatures and lower costs through direct heating and storage of solid particles [1-4]. Commercially available ceramic particles (used in the oil and gas industry for hydraulic fracturing) are inexpensive, durable, and can be heated to temperatures exceeding well over 1000 °C for concentrating solar thermal applications [5].

The conventional particle release pattern in the receiver consists of particles flowing through a single straight discharge slot, forming a planar curtain of particles (Figure 1, left image). This paper introduces new particle release patterns consisting of zig-zag patterns (Figure 1, right image) and multiple parallel particle curtains that can increase light-trapping, reduce radiative and thermal losses, and increase overall thermal efficiency.

Figure 1. Images of conventional straight-line (left) and new zig-zag (right) particle release patterns for falling particle receivers.

A systematic evaluation of non-linear particle release patterns was performed using validated computational fluid dynamics models (ANSYS Fluent) of on-sun tests of a falling particle receiver [6]. Ho et al. [7] introduced square and triangular wave-like particle release patterns. The results of that study indicated that volumetric release patterns could increase the thermal efficiency of the falling particle receiver by up to 7%, and smaller wavelengths and larger amplitudes in the wave-like release patterns resulted in improved performance. This indicated that volumetric (rather than planar) particle releases could benefit the thermal efficiency of particle receivers. The current study introduces multiple parallel particle curtains and includes a parametric study of the impact of particle mass flow rate on the performance of each of the designs. Radiative and convective heat losses are also delineated for each of the particle release patterns in this paper.

MODELING

A drawing of the solid particle receiver and the subsequent Fluent model used in the parametric study is shown in Figure 2 [8]. The Fluent model comprised 169,200 hexahedral cells, which was found to be sufficient to yield convergence in the solutions An air volume was modeled inside the receiver cavity. Cool ambient air entered the domain through the aperture and was circulated through the cavity from interaction with the falling particles or from buoyancy-driven flow resulting from temperature gradients within the air. Turbulent flow was modeled using the realizable k-ε turbulence model and Fluent's standard wall functions. Air left the domain through recirculation out of the aperture or through the bottom outlet, both defined as fixed pressure boundary conditions. The receiver walls were comprised entirely of an alumina silica ceramic fiberboard.

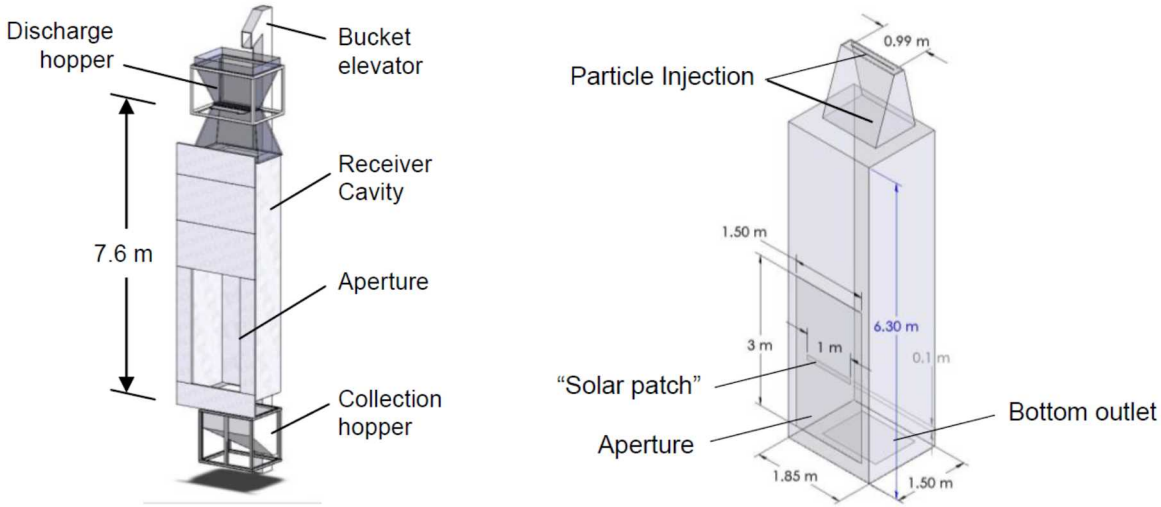

Figure 2. Drawing of the solid particle receiver (left) and the Fluent model used in the parametric study (right) [8].

Particles were released from ~300 injection sites defined near the top of the receiver cavity and tracked through the domain before exiting out the bottom outlet. Each particle's motion was coupled with the air through drag forces acting on the particles. Particle-to-particle interaction was not included under the assumption that the volume fraction of particles in the air volume was sufficiently small. This assumption was valid for volume fractions less than 10%. Previous tests on falling particle receivers have indicated that the volume fraction of particles was less than several percent [9, 10]. Radiative and convective heat transfer to and from the particles was also included in the model.

A non-grey discrete-ordinates radiation model was used to simulate radiation heat transfer inside the domain. Both angular dimensions were discretized into seven divisions. The wavelength spectrum was divided into two spectral bands: 0.1 – 4.5 μm and 4.5 – 100 μm to represent the spectral properties of the receiver walls. All incident solar radiation was defined to enter the domain entirely in the smaller wavelength band (0.1 – 4.5 μm). The higher wavelength band was used to define the emission of thermal radiation from the walls and particles. Incident solar radiation to the domain was applied on a small solar patch within the aperture with an incident power of 1.52×10^{6}

W. An incident beam shape was used with a 30 degree angular range vertically and a 60 degree angular range horizontally that was consistent with the validated model [8].

Conduction through the walls of the receiver was also included in the model in addition to convection on the exterior walls to the surrounding environment. A heat transfer coefficient of 5 W/m^2K was applied on the exterior of the domain for a reference temperature of 300 K. Air entering the domain though the aperture also entered at 300 K.

Thirteen volumetric release patterns were explored in this study including the eight wave-like patterns previously explored in [7]. These configurations are summarized in Table 1. All volumetric release patterns were evaluated against a conventional planar release (labeled as 'Baseline'). Particles from each pattern fell from a 1 m by 0.6 m area near the top of the receiver. The patterns are all 1 m wide, but the depth of each pattern varied and is provided in the table. Approximately 300 injection sites were evenly distributed over the desired pattern, although previous analysis of this model has demonstrated that the number of injection sites does not significantly affect the solution as long as the number of injection sites exceeded 100 [8].

Table 1. Particle-release patterns explored in the study

Case	Depth (m)	Scaled Illustration	Case	Depth (m)	Scaled Illustration
Baseline	N/A		Case 7	0.2	
Case 1	0.4		Case 8	0.2	
Case 2	0.4		Case 9	0.2	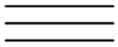
Case 3	0.4		Case 10	0.4	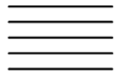
Case 4	0.4		Case 11	0.6	
Case 5	0.2		Case 12	0.4	
Case 6	0.2		Case 13	0.6	

In addition to exploring different types of volumetric release patterns defined in Table 1, each configuration was also simulated at mass flow rates of 3.0, 5.32, 7.0, 10.0, and 12.5 kg/s. Each release pattern explored here was also 1 m in length, so each mass flow rate can also be expressed per unit length (*i.e.* 12.5 kg/s or 12.5 kg/m-s). By varying the mass flow rate, the thermal performance of each volumetric release pattern relative to the baseline configuration was evaluated as the mass flow rate changed. Radiative and convective losses from the model were also computed and summarized for each case.

Figure 3 shows simulated results of the thermal efficiency and radiative losses for the particle release patterns studied, all with the same total mass flow rate. Compared to the baseline (straight-line release pattern), triangular

and square wave-like patterns that had large amplitudes and small wavelengths yielded the highest thermal efficiencies and lowest thermal losses. Multiple parallel curtains also yielded higher thermal efficiencies, and more parallel curtains yielded better performance than fewer curtains. These results indicate that particle release patterns that allow volumetric heating (i.e., heating of particles in the interior regions of the receiver) yield greater light trapping and reduced thermal losses through an insulating effect. The thermal efficiency was strongly correlated to the radiative loss in the solar band (<4.5 μm), indicating that the volumetric particle release patterns increase thermal emission through increased light trapping and reduced solar radiative losses. The relative advantage of these volumetric particle heating designs was greatest at lower mass flow rates (<10 kg/s per meter of slot width) and decreased as the total mass flow rate increased (>10 kg/s per meter of slot width).

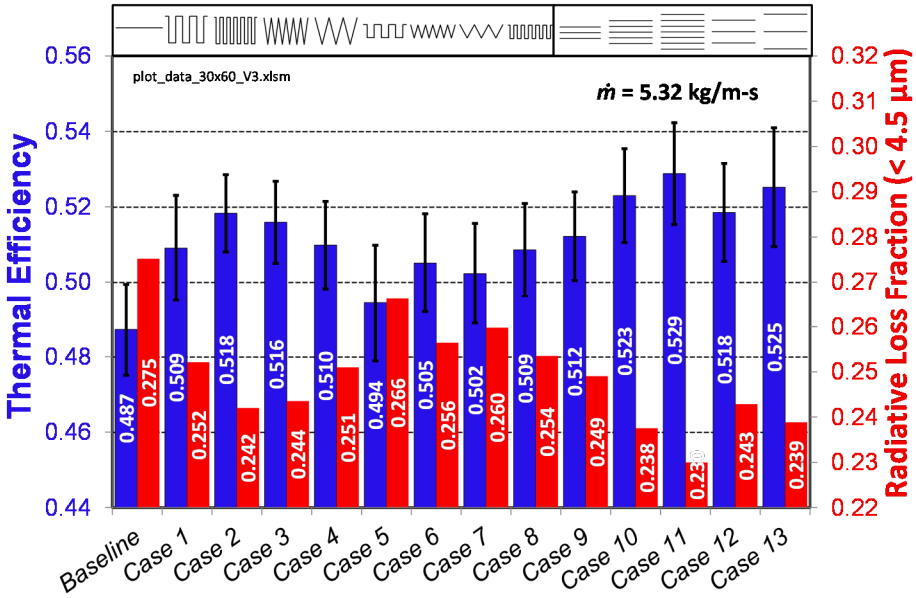

Figure 3. Simulated thermal efficiency and radiative losses for different particle release patterns (indicated above the plot).

The heat losses from all fourteen configurations were calculated for a mass flow rate of 5.32 kg/m-s. The power output from each mechanism was normalized by the total incident radiative power (1.52×10^{6} W) to yield the total percent of incident power lost (Figure 4). Total radiative losses through the aperture and bottom outlet ranged from 27% to 33% with the largest fraction of the radiation leaving the domain having a wavelength < 4.5 μm. Radiative losses were highest in the baseline case. Other losses from the model included convective losses to the air circulating inside the receiver and convective losses to the environment from the exterior walls. Higher convective losses to the air were observed for volumetric release patterns. This was a result of higher particle temperatures and lower particle volume fractions from more distributed particle releases patterns. However, the increased convective losses to the air in the volumetric release patterns were offset by the increased light-trapping effects and lower radiative losses.

The mass flow rate of each particle-release pattern had a significant effect on the thermal efficiency of the receiver. Figure 5 presents the thermal efficiency for cases 2, 3, 9, and 10 as a function of mass flow rate. The mass flow rate was a more significant factor in the thermal efficiency than the particular particle release pattern. Furthermore, diminishing returns were observed in the thermal efficiency as the mass flow rate increased. The normalized thermal efficiency of each case relative to the baseline indicated that as the mass flow rate increased, the relative gains from the volumetric release patterns diminished. It was also observed that for case 1 and case 4, as the mass flow rate approached 12.5 kg/m·s, the volumetric release patterns actually reduced the thermal efficiency relative to the baseline case. Furthermore, as the mass flow rate increased, differences in the thermal efficiency from varying parallel straight-line particle release patterns became less significant. For example, at 12.5 kg/m·s, case 9 with three parallel release lines performed approximately the same as case 11 with seven parallel release lines. Both cases showed only ~2% improvement in thermal efficiency at the highest mass flow rate explored. Likewise at the

highest mass flow rates, the increase in thermal efficiency from spreading out the parallel release lines (case 9 *vs.* case 13) was no longer observed.

Further improvements to the volumetric particle release patterns may be attained by exploring spatial gradients in the mass flow rates. Figure 6 presents a normalized temperature contour plot of the particles leaving the receiver for case 11 with seven parallel release lines at 5.32 kg/m·s and 10.0 kg/m·s. In the figure, the temperature was normalized to the mean particle temperature T_{mean} for each respective flow rate. At lower mass flow rates, the temperature distribution was more uniform compared to higher mass flow rates. At the higher mass flow rates, particle temperatures closest to the incident radiation were hotter and indicated that particles near the rear were being shielded relative to the particles closest to the aperture. Using a spatial gradient in the mass flow rate of the volumetric release patterns such that particles closest to the aperture have a lower concentration could yield a more even distribution in the particle temperatures. Reducing the opacity of the front curtain of falling particles may also reduce reflective losses from the particles closest to the aperture.

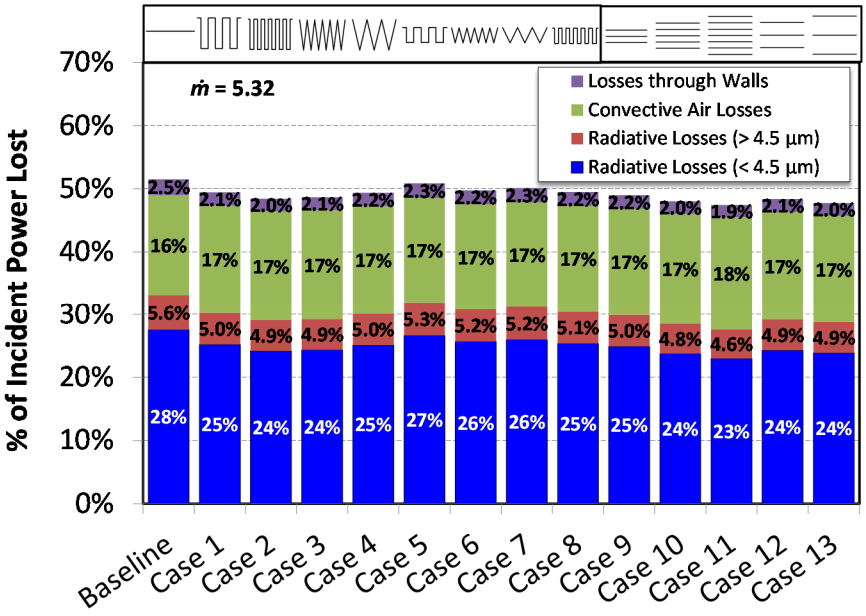

Figure 4. Percent of total incident power lost from each heat-transfer mechanism.

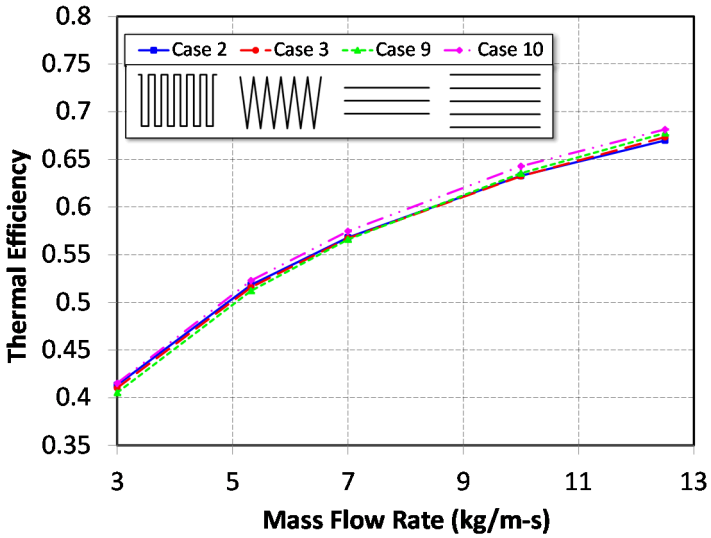

Figure 5. Thermal efficiency for varying mass flow rate for cases 2, 3, 9, and 10.

Future work for this parametric study includes the exploration of gradient mass flow rates on the thermal efficiency and radiative losses. Optimization schemes will be implemented to determine the optimum particle release configuration for different mass flow rates. The distance of the baseline release pattern from the aperture may also be evaluated to determine if location within the receiver has an appreciable effect on thermal efficiency. The proximity of the baseline curtain to the aperture could affect radiative losses that would be reflected or emitted from the walls of the receiver.

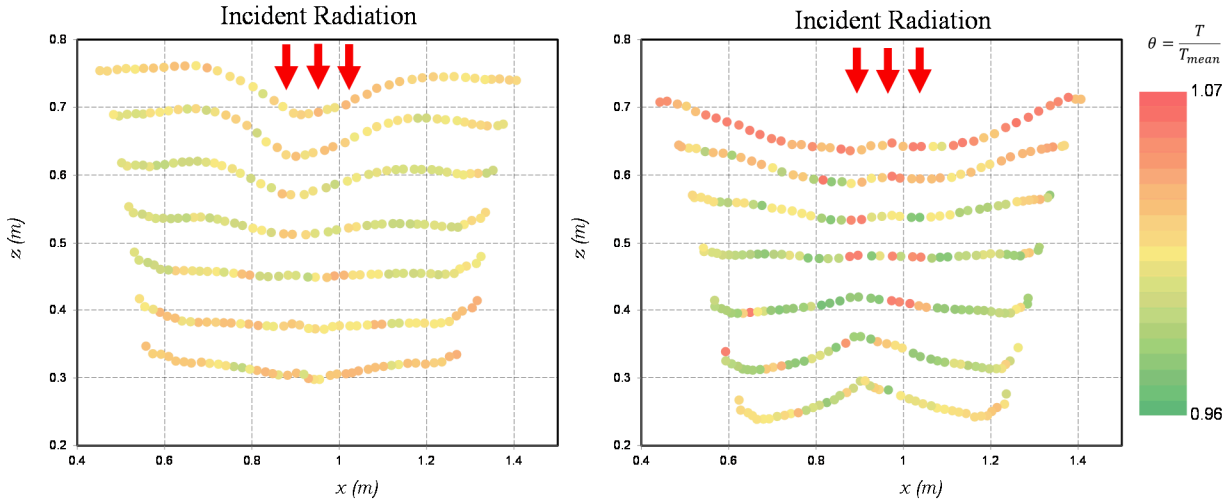

Figure 6. Outlet particle temperatures normalized to their respective minimum temperature forCase 11: 5.32 kg/m-s (left) and 10.0 kg/m-s (right).

TESTING

Particle flow characterization using the alternative particle release patterns has begun using an indoor test apparatus at the National Solar Thermal Test Facility (NSTTF). This apparatus consi sts of a top hopper, open receiver section, bottom hopper, and bucket elevator. The particle drop height is 1.2 m and can accommodate a 1.5 m particle curtain width. The top hopper can hold approximately 1,400 kg of particulate material and currently contains Carbo Accucast ID-50K. The ID-50K particulate material has a mean particle diameter of 280 microns and was utilized in previous on-sun testing at the NSTTF for a full system demonstration of a falling particle receiver [11]. The particle drop is controlled by a discharge plate that is inserted at the bottom of the top hopper. Custom slot apertures corresponding to the different release patterns were cut in the plates. A grid pattern was moved in and out of the particle curtain cross-section to evaluate thickness and offset of the curtain at different locations along the curtain width. Fluorescent lights were installed on either side of the particle curtain to adequately light the grid pattern with uniform, diffuse lighting. Video was taken of the falling particles and then post-processed in a MATLAB code to evaluate particle stability as a function of drop height. The mean and standard deviations of the curtain thicknesses along the drop height were reported for a 15 second drop time.

Sixteen different release patterns were designed and fabricated using 6.35 mm-thick steel plate to structurally accommodate full particle loading from the top hopper. These designs were based on the numerical studies which evaluated linear curtain patterns, triangular wave patterns, square wave patterns, and parallel curtain wave patterns. Each design has a low/high value for wavelength, amplitude, curtain thickness, and/or spacing between multiple parallel curtains. For illustration, a 5-slot parallel curtain design is shown in Figure 7. Each curtain is spaced 4.4 cm apart, and each slot aperture is 6.35 mm. The parallel curtains appear stable in the absence of significant external wind, and the curtain thickness ranged from 1 – 2 cm. The curtain thickness decreases slightly for the first meter of drop, but then began to increase. The decrease in curtain thickness is can be caused by vena contracta (convergence of streamlines exiting a small opening) and/or pressure differentials between the inner and outer regions of the particle curtain as the air is entrained by the falling particles (Bernoulli effect). The higher velocity in the interior causes lower pressure, which causes the particles to converge. However, as the particles accelerate and separate, additional drag causes dispersion and increasing particle curtain thickness. Characterization

of particle flow in the alternative release patterns will be used to determine design criteria that ensure that the desired shape and pattern of the particle curtain is retained over the entire length of the particle drop.

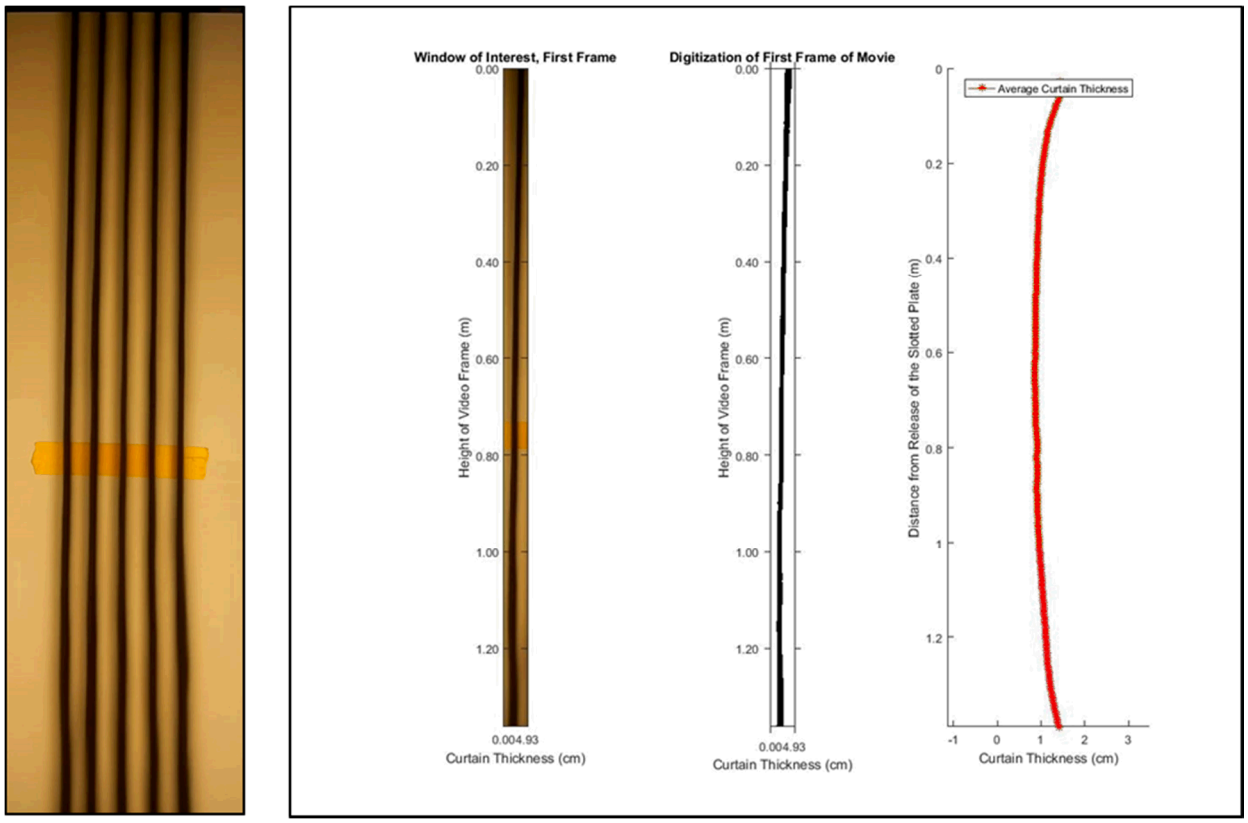

Figure 7. Image of 5 parallel curtains (left) and Matlab analysis of a single curtain from the video (right).

CONCLUSIONS

A parametric study of thirteen different volumetric particle release patterns for a falling-particle receiver was performed using a validated computational fluid dynamics model. Eight "wave-like" release patterns previously investigated of varying amplitude, wavelength, and wave-type and five additional parallel straight-line particle release patterns were compared to a conventional planar release pattern. The mass flow rate of the particle release patterns was evaluated at values of 3.0, 5.32, 7.5, 10.0, and 12.5 kg/m-s, and the relative contribution of heat-loss mechanisms from the domain were delineated.

All volumetric release patterns showed higher thermal efficiencies when compared to the baseline planar particle release pattern with the exception of a few patterns at the highest mass flow rates. Higher thermal efficiencies were associated with lower radiative losses at wavelengths < 4.5 μm, consistent with improved performance in the volumetric release patterns as a result of increased light-trapping effects. The increased light trapping offset increased convective losses due to larger surface areas associated with the volumetric release patterns. Convective losses may play a more significant role at higher temperatures than the ~300 °C achieved in the validated models in the current study. Future simulations will explore higher particle outlet temperatures (>700 °C) and the use of gradients in the mass flow rate of multiple particle curtains to enable greater heating of particles toward the interior of the receiver, which may reduce heat loss through the aperture.

Particle-flow testing has shown that wave-like and multiple parallel curtains can be implemented using various patterns of slotted discharge plates. The pattern of the particle curtains retained their initial shape, despite convective currents that caused some shifting of the curtain position relative to its release point (significant external wind effects were not considered). Candidate release patterns yielding the highest thermal efficiencies and flow stability will be selected for on-sun testing.

ACKNOWLEDGMENTS

Sandia National Laboratories is a multi-program laboratory managed and operated by Sandia Corporation, a wholly owned subsidiary of Lockheed Martin Corporation, for the U.S. Department of Energy's National Nuclear Security Administration under contract DE-AC04-94AL85000.

REFERENCES

1. C. Ho, J. Christian, D. Gill, A. Moya, S. Jeter, S. Abdel-Khalik, D. Sadowski, N. Siegel, H. Al-Ansary, L. Amsbeck, B. Gobereit and R. Buck, *Technology advancements for next generation falling particle receivers*, Proceedings of the Solarpaces 2013 International Conference **49** (Energy Procedia), 398-407 (2014).
2. T. D. Tan and Y. T. Chen, *Review of study on solid particle solar receivers*, Renew Sust Energ Rev **14** (1), 265-276 (2010).
3. C. K. Ho, J. M. Christian, J. Yellowhair, N. Siegel, S. Jeter, M. Golob, S. I. Abdel-Khalik, C. Nguyen and H. Al-Ansary, *On Sun Testing of an Advanced Falling Particle Receiver System*, in *SolarPACES 2015*, Cape Town, South Africa, October 13 - 16, 2015.
4. C. K. Ho, *A Review of High-Temperature Particle Receivers for Concentrating Solar Power*, Appl Therm Eng (in press, available online 3 May 2016: http://dx.doi.org/10.1016/j.applthermaleng.2016.04.103) (2016).
5. N. Siegel, M. Gross, C. Ho, T. Phan and J. Yuan, *Physical properties of solid particle thermal energy storage media for concentrating solar power applications*, Proceedings of the Solarpaces 2013 International Conference **49** (Energy Procedia), 1015-1023 (2014).
6. N. P. Siegel, C. K. Ho, S. S. Khalsa and G. J. Kolb, *Development and Evaluation of a Prototype Solid Particle Receiver: On-Sun Testing and Model Validation*, J Sol Energ-T Asme **132** (2) (2010).
7. C. K. Ho, B. Mills and J. M. Christian, *Volumetric Particle Receivers for Increased Light Trapping and Heating*, in *ASME Power & Energy Conference*, Charlotte, NC, June 26-30, 2016.
8. C. K. Ho, S. S. Khalsa and N. P. Siegel, *Modeling on-Sun Tests of a Prototype Solid Particle Receiver for Concentrating Solar Power Processes and Storage*, in *ES2009: Proceedings of the ASME 3rd International Conference on Energy Sustainability, Vol 2*, San Francisco, CA,
9. N. Siegel, G. Kolb, K. Kim, V. Rangaswamy and S. Moujaes, *Solid particle receiver flow characterization studies*, Proceedings of the Energy Sustainability Conference 2007, 877-883 (2007).
10. C. K. Ho, J. M. Christian, D. Romano, J. Yellowhair and N. Siegel, *Characterization of Particle Flow in a Free-Falling Solar Particle Receiver*, in *Proceedings of the ASME 2015 Power and Energy Conversion Conference*, PowerEnergy2015-49421, San Diego, CA, June 28 - July 2, 2015.
11. C. K. Ho, J. M. Christian, J. Yellowhair, K. Armijo and S. Jeter, *Performance Evaluation of a High-Temperature Falling Particle Receiver*, in *ASME Power & Energy Conference*, Charlotte, NC, June 26-30, 2016.